ELSEVIER

Biophysical Chemistry 90 (2001) 269–277

Biophysical Chemistry

www.elsevier.nl/locate/bpc

# Negative cooperativity and aggregation in biphasic binding of mastoparan X peptide to membranes with acidic lipids

Gerhard Schwarz*, Renate Reiter

*Department of Biophysical Chemistry, Biocenter of the University of Basel, Klingelbergstrasse 70, CH 4056 Basel, Switzerland*

Received 4 December 2000; received in revised form 5 March 2001; accepted 7 March 2001

**Abstract**

The change of Trp fluorescence intensity when large vesicles with 10% acidic lipid are added to mastoparan X solutions reflects a fast and a slow binding process. By means of a novel procedure of data analysis that takes advantage of so-called mass conservation plots we have separated association isotherms related to: (i) the apparent fast pre-equilibrium; and (ii) the final equilibrium, respectively. This approach also reveals that the intrinsic fluorescence signal of the slow binding is considerably raised against that of the fast binding, presumably indicating a penetration of bound peptide from the lipid/water interface into the apolar lipid core. The shape of either binding curve discloses a pronounced tendency of aggregation. Furthermore, it turns out that in the slow process the final binding ratio decreases markedly compared with the initial fast binding ratio. Accordingly the occupation of final binding sites must exert a substantial effect of negative cooperativity on the affinity of the interfacial binding states.


*Keywords:* Peptide–lipid interaction; Membrane biophysics; Electric charge effects; Pore formation; Mass conservation plot; Binding signal analysis

## 1. Introduction

The mastoparan family comprises a number of toxic tetradecapeptides from the venom of various wasp species. They exert manifold biologically significant molecular functions [1–6]. In particular, this includes the generation of a rather pronounced lipid bilayer permeability for hydrophilic substances [5,7–11]. Actually a multitude of other amphiphilic agents, mostly also peptides, induce similar leakage effects in model and cell membranes. Presumably they are caused by the formation of channel-like porous defects in the lipid bilayer structure [12–14]. This could easily be envisaged in terms of the helical bundle ('barrel-stave') model in case that an amphipathic peptide sequence in its α-helical conformation can span the lipid bilayer. Melittin, the major bee

* Corresponding author. Tel.: +41-61-711-4068; fax: +41-61-267-2189.

*E-mail address:* gerhard.schwarz@unibas.ch (G. Schwarz).

0301-4622/01/$ - see front matter 
PII: S0301-4622(01)00149-1

venom factor [15], would comply with this condition whereas the structurally similar mastoparans are definitely not long enough. Nevertheless, both peptide species have been found to show largely the same pore formation pattern with electrically neutral liposomes where the mastoparans only need substantially more material [11] to bring about the same effect as melittin [16].

The underlying molecular mechanism necessarily implies a binding reaction as a first step. This can be monitored by means of an appropriate physical signal, e.g. changes of optical properties such as circular dichroism [17,18] or fluorescence intensity [16,19]. With electrically neutral liposomes the binding does apparently proceed rather fast in the subsecond range [11,16]. In the present study it is demonstrated that the addition of some amount of acidic lipids in the vesicles gives rise to a biphasic binding kinetics. Our fluorescence signal reveals another process in the course of minutes that takes place after the fast phase. This will be shown to arise from a rearrangement of bound peptide which provokes a substantial decrease of the affinity exerted by the initially populated fast binding states. The argumentation takes advantage of a universal model-free approach to analyze binding signals [20]. Such an approach will result in the relevant thermodynamic binding isotherm in any case of a more or less complex molecular mechanism. In particular, structural information about diverse binding states can be derived by investigating the measured signal intensity at equilibrium when being analyzed as a function of the extent of binding.

We consider a total aqueous concentration of peptide, $c_P$, to which vesicles with a lipid concentration, $c_L$, have been added. A partitioning of the peptide between the aqueous and lipid associated moieties will naturally be subject to mass conservation so that

$$c_P = c_f + rc_L \tag{1}$$

involving the concentration of free (i.e. unbound) peptide, $c_f$, and the binding ratio, $r = c_{as}/c_L$ ($c_{as}$ being the concentration of all peptide in a lipid associated state). In the case of equilibrium thermodynamic principles imply a definite functional relationship, the association isotherm (i.e. the so-called 'binding curve')

$$r = f(c_f) \tag{2}$$

It is determined by the underlying molecular binding mechanism. With a series of different $c_P$ one can find matching $c_L$-values where the related $r$, $c_f$ remain the same. According to Eq. (1) a plot of these $c_P$ vs. those $c_L$ must fit a straight line whose intercept and slope are equal to $c_f$ and $r$, respectively. Such a procedure may be realized in general practice with an appropriate binding signal [20].

In the present case we measure the fluorescence intensity, $\Phi$, emitted by the Trp residue in the mastoparan X peptide under investigation. Intrinsic molar intensities of free and any number of bound peptide states $i$ ($= 1, 2, \ldots$) are taken into account as constant coefficients $\varphi_o$, $\varphi_i$ so that

$$\Phi = \varphi_o c_f + \Sigma_i \varphi_i c_i \tag{3}$$

is a linear function of the diverse individual peptide concentrations. The pertinent experimental binding signal $F = \Phi - \Phi_o$ ($\Phi_o = \varphi_o c_P$) is then chosen to be the change of $\Phi$ when lipid has been added to a pure peptide solution. This is readily expressed as

$$F = F_\infty r c_L \tag{4a}$$

involving a characteristic molar signal intensity

$$F_\infty = \Sigma_i \Delta\varphi_i x_i \tag{4b}$$

($\Delta\varphi_i = \varphi_i - \varphi_o$; $x_i = c_i/c_{as}$). At equilibrium it is functionally determined by $r$ which plays the role of a single independent thermodynamic variable of state. Note that $F_\infty$ would be a constant upon more or less binding only if either any bound molecule emits the same intrinsic signal or the molar fractions of bound molecules in their various possible states remain unaltered. Otherwise a change of $F_\infty$ with $r$ discloses quantitative infor-

mation about structural transitions between different binding modes in the course of the binding process.

According to Eq. (4b) we may evaluate from the experiments the quantity

$$Q(r) = F/c_L = F_\infty(r)r \tag{4c}$$

in a series of measurements with sufficiently different $c_P$ to which more and more lipid is added. Pairs of matching $c_P$, $c_L$ (at a given value of $Q$) can so be determined where according to Eq. (2) both $r$ as well as $c_f$ must each be on the same level. These $c_P$ and $c_L$ can then be utilized for a linear mass conservation plot according to Eq. (1). Since the basic idea of this approach was first published [21,22] only overall binding curves have sporadically been derived in this way. As pointed out quite recently [20] the method under consideration also implies a highly useful potential to differentiate between diverse binding states by means of analyzing $F_\infty(r)$. We shall demonstrate this in the present article. It is shown that the binding affinity of rapidly bound molecules is substantially reduced by peptide in slowly populated binding states which has apparently farther penetrated the lipid membrane.

## 2. Materials and methods

### 2.1. Peptide

All experiments were performed with synthetic mastoparan X having the amino acid sequence $^{+}$INW$^{+}$KGIAAM$^{+}$K$^{+}$KLL–$NH_2$. It was supplied by Bachem Feinchemikalien (Bubendorf BL, Switzerland). The concentration of the aqueous peptide solution was determined by measuring the tryptophan absorption with an UV spectrometer ($\lambda = 280$ nm, $\varepsilon = 5570\ cm^{-1}\ M^{-1}$). Small amounts of stock solution were stored at $-20$°C.

### 2.2. Lipid vesicles

The phospholipids were purchased from Avanti Polar Lipids (Birmingham, AL, USA). A mixture of 90 wt.% POPC and 10 wt.% POPS dissolved in chloroform was pre-dried under a flow of nitrogen gas and dried under oil pump vacuum for 3 h. The lipid film was dissolved in an aqueous buffer containing 10 mM Hepes (Bioprobe, France), 107 mM sodium chloride (Merck), 1 mM EDTA (Merck) and 5.6 mM sodium hydroxide to adjust the pH value to 7.4. The lipid suspension was vortexed for approximately 3 min and then subjected to five freeze–thaw cycles in liquid nitrogen. The solution was extruded 10 times through a stack of two polycarbonate membranes with a pore size of 100 nm (Nucleopore, Sterico) at a nitrogen pressure of 15 bar. The exact concentration of the lipid solution was determined by phosphate analysis [23]. Dynamic light scattering experiments with a commercial supplier ALV 5000 at $\lambda = 532$ nm and various detection angles between 30° and 150° were performed to determine the size of the vesicles. The size distribution of the diameter turned out to be very narrow having a maximum at 106 nm (with a polydispersity parameter $\beta$ of 0.964, compared with 1.0 for a perfectly monodisperse system).

### 2.3. Fluorescence measurements

The experiments were carried out on a spectrofluorometer F777 (Jasco, Tokyo, Japan) equipped with one monochromator in each light path. The excitation wavelength was set at 280 nm (bandwidth: 1.5 nm) and the emission wavelength was 325 nm (bandwidth: 3 nm). This corresponds to the peak of the Trp spectrum of the bound molecule. Details of whole spectra changes were not needed in our present analytical approach. Quartz cuvettes with a path length of 1 cm were used. The temperature was kept constant at 20°C. Each peptide concentration was adjusted in a separate vessel and used for the whole series of concentrations. Lipid vesicles were titrated into the peptide solution while stirring and measuring continuously. An implied dilution was taken into account upon fixing the actual values of $c_P$ and $c_L$. The fluorescence signal was measured as a function of time and corrected for light scattering effects [19]. Its increase apparently reflects bound peptide where the Trp fluorophore has pene-

trated an environment of reduced polarity at or inside the lipid moiety.

## 3. Results

Solutions of mastoparan X in our standard buffer have been examined at concentrations of $c_P$ $\mu M^{-1} = 4.5$, 6.7, 10 and 14, respectively. In each case the fluorescence intensity $\Phi$ was recorded in the course of time $t$ after an addition of lipid vesicles. A typical example of such a recording is presented in Fig. 1. There is a practically instantaneous initial jump of $\Phi$ up to $\Phi'$ above its zero value $\Phi_o$ (in a pure peptide solution). The so established signal $F' = \Phi' - \Phi_o$ is considered to reflect a fast pre-equilibrium of binding. Subsequently a comparatively slow increase of $\Phi$ is observed. It approaches asymptotically a level of $\Phi''$ which results in a signal $F'' = \Phi'' - \Phi_o$, related to a slowly established apparently final equilibrium. A plot of log $(\Phi'' - \Phi)$ vs. $t \rightarrow 0$ leads to a rather well founded $Q'$-value whose remaining small uncertainty does not essentially affect the binding curves.

Firstly, we examine $Q' = F'/c_L$ as it decreases for a given $c_P$ upon adding more and more lipid vesicles. This is shown in Fig. 2a for each of the $c_P$ under consideration. In a double logarithmic plot the measured data can be fitted quite satisfactorily by straight lines. At fixed values of $Q'$ in the range of 12 down through 4 (expressed in a.u. $\mu M^{-1}$) we have evaluated the corresponding $c_L$ for the various $c_P$ which yields four points for a mass conservation plot. Several examples are displayed in Fig. 2b. According to the Eqs. (1) and (4c) this leads to $r$, $c_f$, and $F_\infty' = Q'/r$. Secondly, an analogous procedure was carried out with the final quantity $Q''$ as to be seen in the Fig. 3a,b.

Let us now envisage Fig. 4 where both the

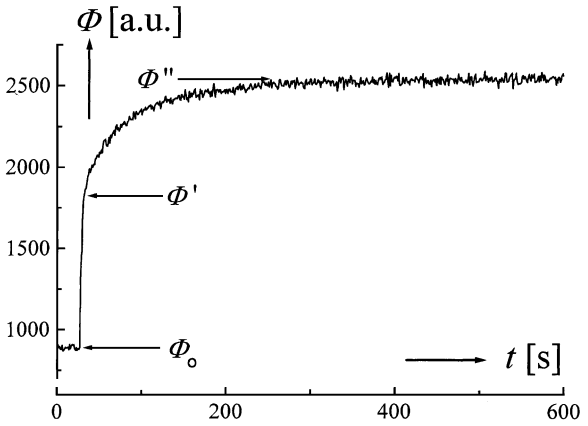


Fig. 1. Typical example of the course of fluorescence intensity $\Phi$ (arbitrary units) after having added lipid vesicles to an originally pure mastoparan X solution ($c_P = 10$ $\mu M$, $c_L = 161$ $\mu M$). There is a practically instantaneous jump from $\Phi_o$ (being corrected for dilution) up to $\Phi'$ that is followed by a slow approach to a final value $\Phi''$.

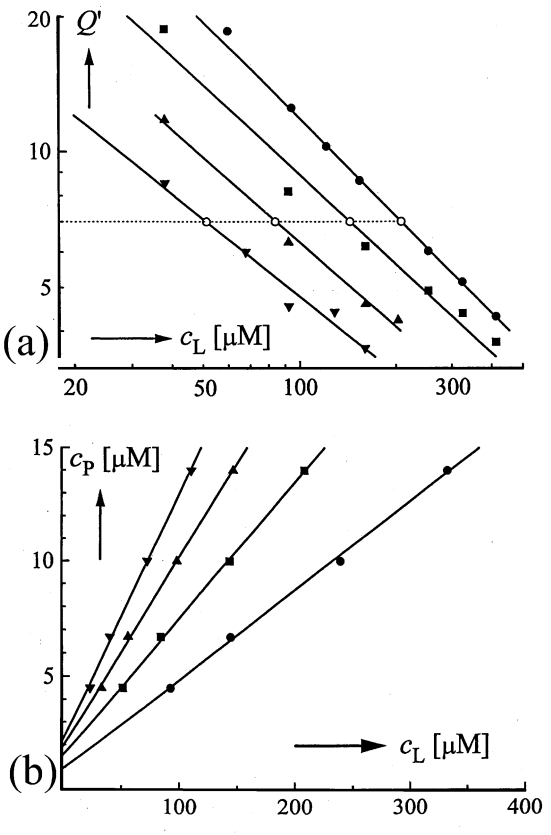


Fig. 2. Evaluation of data at fixed $Q'$ (see text). (a) Double logarithmic plots of $Q'$ vs. $c_L$ for various peptide concentrations $c_P$ $\mu M^{-1} = 4.5$ (▼), 6.7 (▲), 10 (■), 14 (●). The dashed horizontal line at $Q' = 7$ a.u. $\mu M^{-1}$ exemplifies points (○) with matching $c_P$, $c_L$-pairs for a mass conservation plot [according to Eq. (1)]. (b) Examples of such linear plots for $Q'$ (in a.u. $\mu M^{-1}$) = 5 (●), 7 (■), 9 (▲), 11 (▼) resulting in $c_f$ (intercept) and $r$ (slope), respectively.

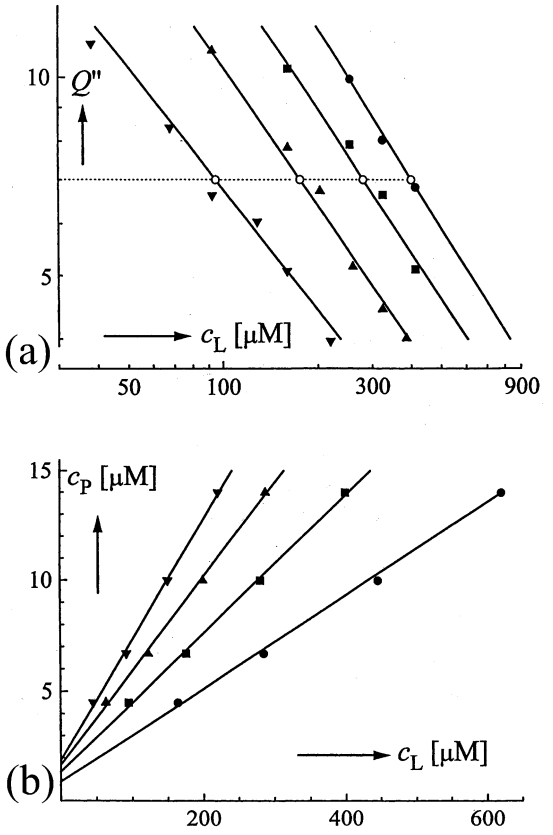


Fig. 3. Evaluation of data at fixed $Q''$ (see text) analogously as done in Fig. 2 with $Q'$.

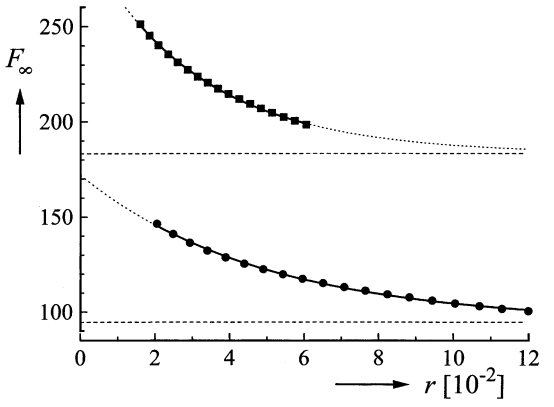


Fig. 4. The characteristic fluorescence intensity $F_\infty$ (in a.u. $\mu M^{-1}$) for the fast (●) as well as the final (■) states of bound peptide. The data points are fitted by single exponential curves (dotted) of the form $A + B \times \exp(-r/C)$ where A = 94.6, 183.3; B = 77.3, 113.1; $C = 4.85 \times 10^{-2}$, $3.06 \times 10^{-2}$, respectively.

characteristic $F_\infty$-terms are presented as a function of the binding ratio. We should emphasize that $F_\infty$ [see Eq. (4b)] must remain constant if the emitted fluorescence of bound peptide is the same in any of its possible states. Obviously our results demonstrate a very pronounced increase of the fluorescence intensity when the slowly populated binding sites are finally occupied. However, there is a creeping decrease of the characteristic signal for the fast as well as the final binding states, indicating some molecular interaction that causes a quenching effect.

The two binding isotherms in Fig. 5 also feature a qualitatively similar appearance. There is a linear increase up to approximately 1.3 μM of free peptide reflecting thermodynamically ideal binding conditions, described by $r = K_p c_f$ with a partition coefficient $K_p = 3.9 \times 10^4$ ($\pm 0.3$) $M^{-1}$ for the fast and $K_p = 2.25 \times 10^4$ ($\pm 0.3$) $M^{-1}$ for the final binding. The uncertainty of roughly 10% is essentially due to an error margin of some $\pm 0.1$ μM in the determination of $c_f$ from the intercept of the mass conservation plots. The slope is much less error affected so that $r$ and $F_\infty$ can be evaluated more precisely.

Beyond the ideal range of binding the upward

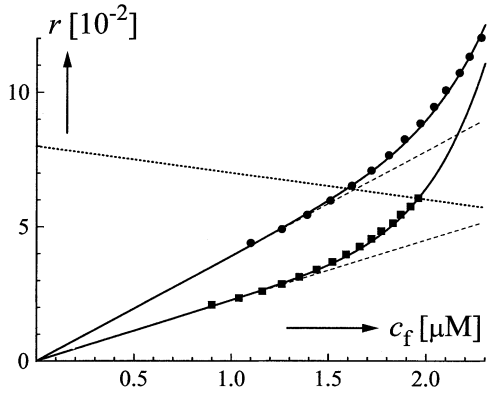


Fig. 5. Binding isotherms plotted as $r$ vs. $c_f$. The points are fitted according to an octameric micellation model by a function of the type $A \times c_f + B \times c_f^8$ with $A = 3.9 \times 10^{-2}$, $B = 4.5 \times 10^{-5}$ (●, fast equilibrium) and $A = 2.25 \times 10^{-2}$, $B = 7.5 \times 10^{-5}$ (■, final equilibrium) where $c_f$ is expressed in μM units. For details see text.

curvature indicates some attractive interaction, presumably aggregation of bound peptide. As a rather unexpected peculiar finding we observe a decrease of the total binding in the course of the slow process.

## 4. Discussion

Binding of the mastoparans as well as of the structurally analogous amphipathic melittin to electrically neutral lipid vesicles is very rapidly completed in the subsecond range [11,16]. This appears to be a nearly diffusion-limited process [18,24]. Experimental evidence indicates that the bound mastoparan molecules on neutral lipid membranes assume a largely helical conformation [25] oriented parallel on the outer surface [26] similar to melittin which is likewise surface seeking according to a hydrophobic moment analysis [27]. Our present results with mastoparan X and negatively charged liposomes (10% acidic lipids) also reveal such a fast binding step being followed, however, by another comparatively slow change of the binding signal. We reason that in this case a similar surface association occurs leading to a fast pre-equilibrium. In view of Eq. (4b) the decrease of the characteristic binding signal $F_\infty'(r)$ exhibited in Fig. 4 points to a pronounced distribution of the individual binding states. Such could be caused upon more and more crowding so that the Trp residue is gradually pushed into a domain of higher polarity (towards the aqueous moiety) and/or by quenching due to the formation of aggregates. Aggregation is actually supported by the upward curvature of the binding isotherm in Fig. 5. It may be well fitted on the basis of a broad variety of conceivable quantitative models that could be more or less complex. In order to demonstrate this most simply we confine ourselves to a thermodynamic ideal formation of uniform aggregates. A best fit is then obtained assuming octameric micellation according to

$$r_8 = K_8 r_1^8 \tag{5}$$

if we presume an ideal monomer–monomer partitioning with $r_1 = K_p c_f$ as indicated by the linear part of the binding curve (see slope of the dashed line in Fig. 5). The partition coefficient $K_p = 3.9 \times 10^4\ M^{-1}$ is approximately a factor of 10 larger than determined for mastoparan X with neutral liposomes [11]. This factor $\kappa$ can be considered to result from the electrostatic attraction that the negative electric potential of the lipid surface exerts on the positive peptide charges. Based on the Gouy–Chapman model one obtains

$$k = \exp\{2z\sinh^{-1}(\gamma b)\} \tag{6}$$

with $z$ = effective charge number per peptide monomer, $\gamma$ = fraction of effective negative charge per lipid molecule, $b = 11.5$ (according to the physical characteristics of the aqueous electrolyte [11]). A value of $\gamma = 0.1$ corresponding to the actual fraction of acidic lipid would imply $z = 1.2$ which is, however, much smaller than the 2.4 that was found in the neutral lipid case [11]. Even that is markedly below the intrinsic physical charge number of almost 4 at the given pH. This well-known phenomenon has been attributed to deficiencies in the application of the Gouy–Chapman model which is based on a smeared out charge density in the very two-dimensional interface between the polar buffer and apolar lipid moieties [28].

In reality, we have, however, a distribution of discrete charges extending to some degree in the three-dimensional surroundings. Under such circumstances the effective charges will actually become reduced. Thus also the $\gamma$-term may be affected. Keeping $z = 2.4$ the observed $\kappa$-factor leads to $\gamma = 0.043$. Anyway, there is in addition the possibility that charges are neutralized due to p$K$-shifts because of low dielectric constants. We note that even with electrically neutral lipid membranes initially linear association isotherms exhibiting subsequent upward curvature have been observed if only the positive charges on the peptide are comparatively small as for instance in the case of polistes mastoparan [11] or alamethicin [21]. In view of these rather complex electrostatic features the present value of $K_p$ appears to be quite reasonable. Nevertheless, we cannot definitely rule out possible stronger attraction at low

$c_f$ because of missing reliable data (due to the uncertainty of the intercept in the mass conservation plots). At any rate, the apparent upward curvature of the binding isotherm must be taken into account as an indication of aggregation above a specific critical concentration. According to Fig. 5 this becomes evident at approximately $r = 0.06$ pointing to the formation of larger aggregates although their actual dispersion cannot be clearly deduced. The possible formation of octamers implies the existence of equal amounts of monomeric and aggregated peptide at $r \approx 0.2$ (corresponding to a molecular ratio of 1:5 peptide per lipid).

The slow increase of the fluorescence binding signal may at first sight be regarded as an indication of additional peptide being bound. This would certainly be correct if the newly assumed binding states emit the same intrinsic fluorescence intensity as the rapidly occupied states. However, such conditions must not simply be taken for granted. Application of our data analysis enables us to separate quantitatively the fast and the final binding characteristics. Accordingly we observe that the average molar fluorescence intensity is substantially increased once the slow process has reached its final equilibrium. In the course of it new binding states are obviously occupied which feel a further reduced environmental polarity, presumably because the peptide has penetrated farther into the hydrophobic core of the lipid bilayer. This appears to be associated with extensive translocation across the membrane as indicated by pertinent chemical evidence [11].

We note that the established slow binding isotherm exhibits qualitatively the same shape that was already seen in the fast case, i.e. an initial linear part followed by an upward curvature that can as well be fitted by an octameric micellation model (see Fig. 5). It must be considered to reflect a superposition of signals sent forth by both fast and slowly bound peptide. Surprisingly, the total binding ratio is found to be smaller than in the initial fast binding event. This implies a pronounced effect of negative cooperativity being exerted on the surface binding. Thus the underlying displacement of peptide into the more apolar interior of the membrane does substantially impair the surface binding affinity. We gather that farther penetrated positive peptide charges have to a considerable degree neutralized the negative lipid charges so that the electrostatic factor $\kappa$ is reduced. For given $c_P$, $c_L$ the mass balance relation of Eq. (1) may be plotted in the $r$ vs. $c_f$ diagram as a straight line. Its intersection points with the specific binding curves permit a quantitative analysis of the change of binding states in the course of the slow process. As an example we present the case of $c_P = 8$ μM, $c_L = 100$ μM as a dotted line in Fig. 5. One observes a decrease of the binding ratio $r = 0.064$ at the surface to a total of 0.0605 together with the slowly occupied binding states indicating that the surface binding must be substantially reduced. Also we note an increase of $c_f$ from 1.6 to 1.96 μM. Interestingly, on the other hand, it turns out that the fraction of aggregated peptide has grown from nearly nothing to approximately 26% of bound material.

The binding isotherm of mastoparan X with neutral liposomes had not indicated noticeable aggregation. Nevertheless, the apparent pore formation pattern revealed that rather small amounts of peptide could penetrate the core of the lipid bilayer during an initial short period of structural perturbation so that transient pore-like aggregates are formed [11]. The presence of negative charges appears to reduce the overall net charge density sufficiently so that aggregation is substantially promoted and can be seen directly in the upward curvature of the binding isotherm. Actually this phenomenon had been observed with neutral liposomes if only the peptide ligand carried comparatively little positive charge as was demonstrated in the case of polistes mastoparan (only two basic residues). This had also led to a strongly intensified pore formation process [11]. The possible effect of aggregation on pore formation in our present system remains to be investigated in further studies.

## 5. Conclusions

Data analysis using mass conservation plots could well be applied to separate fluorescence signals and binding curves of a fast transient

pre-equilibrium and the final equilibrium, respectively, exhibited by the present biphasic peptide-liposome binding process.

The fast phase does apparently result from a nearly diffusion controlled association of the positively charged peptide at the lipid/water interface as it takes place with electrically neutral vesicles as well. However, in comparison with the latter case, the presence of negative lipid charges does strongly raise the binding affinity and promote aggregation of bound mastoparan X molecules.

In the final course of the binding reaction the peptide is seen to penetrate farther into the more apolar interior of the lipid bilayer while aggregation still increases. This proves to have a significant effect of negative cooperativity on the fast surface binding so that the total binding ratio is actually reduced.

## Acknowledgements

This work has been supported by the Swiss National Science Foundation grant no. 31-42045.94.

## References

[1] Y. Hirai, T. Xasuhura, H. Yoshida, T. Nakajima, M. Fujino, C. Kitada, A new mast cell degranulation peptide 'mastoparan' in the venom of *Vespula lewisii*, Chem. Pharm. Bull. 27 (1979) 1942–1944.

[2] Y. Hirai, M. Kuwada, T. Yasuhura, H. Yoshida, T. Nakajima, A new mast cell degranulating peptide homologous to mastoparan in the venom of Japanese hornet (*Vespa xanthoptera*), Chem. Pharm. Bull. 27 (1979) 1945–1946.

[3] Y. Hirai, Y. Ueno, T. Yasuhura, H. Yoshida, T. Nakajima, A new mast cell degranulating peptide, polistes mastoparan, in the venom of *Polistes jadwigae*, Biomed. Res. 1 (1980) 185–187.

[4] T. Higashijima, S. Uzu, T. Nakajima, E.M. Ross, Mastoparan, a peptide toxin from wasp venom, mimics receptors by activating GTP-binding regulatory proteins (G-proteins), J. Biol. Chem. 263 (1988) 6491–6494.

[5] A. Argiolas, J.J. Pisano, Facilitation of phospholipase A2 activity by mastoparans, a new class of mast cell degranulating peptides from wasp venom, J. Biol. Chem. 258 (1983) 13697–13702.

[6] P.J. Weidmann, W.M. Winter, The G-protein-activating peptide mastoparan and the synthetic $NH_2$-terminal ARF peptide ARFp13 inhibit in vitro Golgi transport by irreversibly damaging membranes, J. Biol. Chem. 127 (1994) 1815–1827.

[7] T. Katsu, M. Kuroko, T. Morikawa, K. Sanchike, H. Yamanaka, S. Shinoda, Y. Fujita, Interaction of wasp venom mastoparan with biomembranes, Biochim. Biophys. Acta 1027 (1990) 185–190.

[8] D.R. Pfeiffer, T.I. Gudz, S.A. Novgorodov, W.L. Erdahl, The peptide mastoparan is a potent facilitator of the mitochondrial permeability transition, J. Biol. Chem. 270 (1995) 4923–4932.

[9] A. Arbuzova, G. Schwarz, Pore kinetics of mastoparan peptides in large unilamellar lipid vesicles, Progr. Colloid Polym. Sci. 100 (1996) 345–360.

[10] I.R. Mellor, M.S.P. Sansom, Ion channel properties of mastoparan, a 14-residue peptide from wasp venom, and of MP3, a 12-residue analogue, Proc. R. Soc. (Lond.) B 239 (1990) 383–400.

[11] A. Arbuzova, G. Schwarz, Pore forming action of mastoparan peptides on liposomes. A quantitative analysis, Biochim. Biophys. Acta 1420 (1999) 139–1152.

[12] M.S.P. Sansom, The biophysics of peptide models of ion channels, Progr. Biophys. Mol. Biol. 55 (1991) 139–235.

[13] D.M. Ojcius, J.D.-E. Young, Cytolytic pore forming proteins and peptides: is there a common structural motif? Trends Biochem. Sci. 16 (1991) 225–229.

[14] D. Marsh, Peptide models for membrane channels, Biochem. J. 315 (1996) 345–361.

[15] C.E. Dempsey, The action of melittin on membranes, Biochim. Biophys. Acta 1031 (1990) 143–161.

[16] S. Rex, G. Schwarz, Quantitative studies on the melittin-induced leakage mechanism of lipid vesicles, Biochemistry 37 (1998) 2336–2345.

[17] G. Schwarz, U. Blochmann, Association of the wasp venom peptide mastoparan with electrically neutral lipid vesicles, FEBS Lett. 318 (1983) 172–176.

[18] G. Schwarz, G. Beschiaschvili, Thermodynamic and kinetic studies on the association of melittin with a phospholipid bilayer, Biochim. Biophys. Acta 979 (1989) 82–90.

[19] N. Hellmann, G. Schwarz, Peptide-liposome association. A critical investigation with mastoparan X, Biochim. Biophys. Acta 1369 (1998) 267–277.

[20] G. Schwarz, A universal thermodynamic approach to analyze biomolecular binding experiments, Biophys. Chem. 86 (2000) 119–129.

[21] G. Schwarz, H. Gerke, V. Rizzo, S. Stankowski, Incorporation kinetics in a membrane, studied with the pore forming peptide alamethicin, Biophys. J. 52 (1987) 685–692.

[22] W. Bujalowski, T.M. Lohman, A general method of analysis of ligand-macromolecular equilibria using a spectroscopic signal from the ligand to monitor binding. Application to Escherichia coli single strand binding protein-nucleic acid interactions, Biochemistry 26 (1987) 3099–3106.

[23] C.J.F. Böttcher, C.M. Van Gent, C. Fries, A rapid and sensitive sub-micro phosphorous determination, Anal. Chim. Acta 24 (1961) 203–204.
[24] K.M. Sekharam, T.D. Bradrick, S. Georghiu, Kinetics of melittin binding to phospholipid small unilamellar vesicles, Biochim. Biophys. Acta 1063 (1991) 171–174.
[25] T. Higashijima, K. Wakamatsu, M. Takemitsu, M. Fujino, T. Nakajima, T. Miyazawa, Conformational change of mastoparan from wasp venom on binding with phospholipid membrane, FEBS Lett. 152 (1983) 227–230.
[26] K. Fujita, S. Kimura, Y. Imanishi, Self-assembly of mastoparan X derivative having fluorescence probe in lipid bilayer membrane, Biochim. Biophys. Acta 1195 (1994) 157–163.
[27] D. Eisenberg, E. Schwarz, M. Komaromy, R. Wall, Analysis of membrane and surface protein sequences with the hydrophobic moment plot, J. Mol. Biol. 179 (1984) 125–142.
[28] S. Stankowski, Surface charging by large multivalent molecules. Extending the standard Gouy–Chapman treatment, Biophys. J. 60 (1991) 341–351.